Bulletin of the Geological Society of Malaysia, Volume 71, May 2021, pp. 185 - 202
DOI: https://doi.org/10.7186/bgsm71202115

Late Pleistocene climate variation on the Khorat Plateau, northeastern Thailand inferred from the remnants of sand dunes

Patcharaporn Ngernkerd[1], Montri Choowong[1,*], Nutcha Choowong[2], Peerasit Surakiatchai[1]

[1] Morphology of Earth Surface and Advanced Geohazards in Southeast Asia Research Unit (MESA RU), Department of Geology, Faculty of Science, Chulalongkorn University, Bangkok 10330, Thailand
[2] Chulalongkorn Demonstration School, Faculty of Education, Chulalongkorn University, Bangkok 10330, Thailand
* Corresponding author email address: Montri.c@chula.ac.th

Abstract: The preservation of terrestrial dune field in a tropical region is rare and relies significantly on the degree of weathering process, humidity and anthropogenic condition. In this paper, we report the remnants of sand dunes that is uncovered from Thungkula Ronghai (TKR) dune field in the southern part of the Khorat Plateau, northeastern Thailand. We reveal, for the first time, the results of systematic geomorphological, sedimentological and chronological analyzes of barchanoid ridges and parabolic dunes found on terraces of the Mun and the Chi Rivers. Interpretation in a series of 1952 aerial photographs, satellite images coupled with Ground Penetrating Radar (GPR) survey, and optically stimulated luminescence (OSL) dating were applied. As a result, we found remnants of mega-barchanoid ridges and isolated parabolic dunes varying in height from 1-2 m with maximum length of 4 km, locally distributed in between terraces of the Mun and Chi Rivers, the middle to eastern part of TKR. Dune shapes include lobate, en-echelon and elongate partially overlying on crevasse sand splay, meandered scar, paleo-channel, mid-channel bar of the fluvial depositional sequences. Orientation of all dunes is in NW-SE direction reflecting the formation was due to the prevailing NW monsoon wind. Transition from barchanoid ridge to parabolic dune was observed. Preliminary OSL dating reveals the deposition of sand dunes occurred between 45 to 28 ka. This age range can be inferred to a warmer and drier period occurred in Marine Isotope Stage 3 (MIS3) before the Last Glacial Maximum.

Keywords: Parabolic dune, barchanoid ridges, sand splay, Chi River, Khorat Plateau, TKR

INTRODUCTION

Sand dune is one of spectacular landforms on earth that is widely distributed around the world's deserts and coastlines. The formation processes and classification of sand dunes on Earth and Mars have been studied since the past decades. In general, aeolian desert and coastal sand dune types were classified as shadow dune, barchan, parabolic, barchanoid ridge, linear, transverse and star dunes (Pye, 1993). Hack (1941) defines parabolic dunes as long, scoop hollows, or parabolas of sand, with points tapering to windward; with a much gentler windward slope than leeward slope. Parabolic dunes are U or V shaped dunes that develop a form which is, wholly, or in part controlled by the stabilization of vegetation (Landsberg, 1956; Jennings, 1957). A parabolic dune is consisting of at least three basic features, a depositional lobe (formerly defined as a precipitation ridge marking the extent of dune migration (Cooper, 1958), trailing arms or ridges, and a deflation basin (McKee, 1979; Thompson, 1983). McKee (1979) classified sand dunes based on a combination of shape, number and orientation of slip-faces close to the prevailing wind or sand drift direction, and degree of form mobility. The depositional lobe can be defined as a mound of active to partially vegetated sand on the downwind extent of the dune (Thompson, 1983). Lancaster (2014) suggested that the simplest dune types and patterns can form in areas characterized by a narrow range of wind directions (unidirectional wind regime). Barchanoid ridge is asymmetrical wavy dune ridge consisting of parallel rows of coalesced barchans (connected crescents). Barchanoid ridges display as a downwind-facing barchanoid followed by an upwind-facing linguoid element (Tirsch, 2014). It is oriented transverse to the predominant wind direction and migrates forward. It has gently dipping windward slopes and steeply dipping leeward slopes. In the absence of vegetation, crescentic dunes will be the dominant form. Isolated crescentic dunes, or barchans, occur in areas of limited sand supply; they coalesce laterally to form crescentic (barchanoid) ridges as sand supply increases. Parabolic dunes are oval shaped features with a ring of sand along the leeward side and with wings open towards the windward opening (Melton, 1940). In wet aeolian systems, the water table is at or near the surface and so controls accumulation dynamics. Where vegetation controls accumulation dynamics, the system is known as a stabilizing aeolian system (Lancaster, 2014).

Aeolian dune formation can infer the difference in climate conditions (e.g. cold and warm, wet and dry), sources of sediment supply and vegetation. In general, the terrestrial and surficial landforms, especially sand dune, formed during the Pleistocene were not well preserved due to its sensitivity to the weathering and erosion processes and anthropogenic disturbance. In particular, a tropical region where the rainfall and humidity play significant role, the discussion on the past climate changes has been relied mainly on the analysis of geological archives such as marine and lake sediments, and speleothems (Chabangborn & Wohlfarth, 2014 ; Chawchai *et al*., 2018). Here we show, for the first time, the uncovering of terrestrial sand dune as evidence for inferring the late Pleistocene climate variation in the region. Apart from loess that has been analyzed from several locations in northeastern Thailand (e.g. Phien-wej *et al*., 1992; Nichol & Nichol, 2013), sand ridge deposited on paddy field (Pramojanee *et al*., 1985) non-organic aeolian sand deposits (Loffler *et al*., 1984) and sand splay (Hokjaroen, 1989; Parry, 1990) were reported. However, none of the detail geological and geomorphological analyzes in the aeolian sand dune in Thungkula Ronghai (TKR) has been carried out. Here in this paper, we reveal our findings and discuss the process of sand dune formation discovered on a surface of terraces of the Mun and Chi Rivers in the TKR dune field, south-eastern part of the Khorat Plateau. The study area covers part of Yasothon, Srisaket and Ubon Ratchathani provinces (Figure 1). We described and criticized in detail the morphology of dunes coupled with their stratigraphy and chronology in order to understand how they formed and discuss what do we learn from this rare terrestrial preservation.

Remnants of parabolic dunes and barchanoid ridges were preserved in TKR. The difficulty to recognize them is that parts of their morphology were eroded, high-vegetated. The availability to conduct detail geomorphological and geophysical survey is only in the low- or none-vegetated dune field. Recently, they are overlying on floodplain and abandoned channel of the Chi River. Thus, we used ground penetrating radar (GPR) in order to differentiate dune stratigraphy from fluvial deposits. Optically stimulated luminescence (OSL) were applied to date the age of sand dune and fluvial deposit along with GPR survey line. GPR can detect differences such as compaction and/or water content, allowing stratigraphy to be more obvious in the

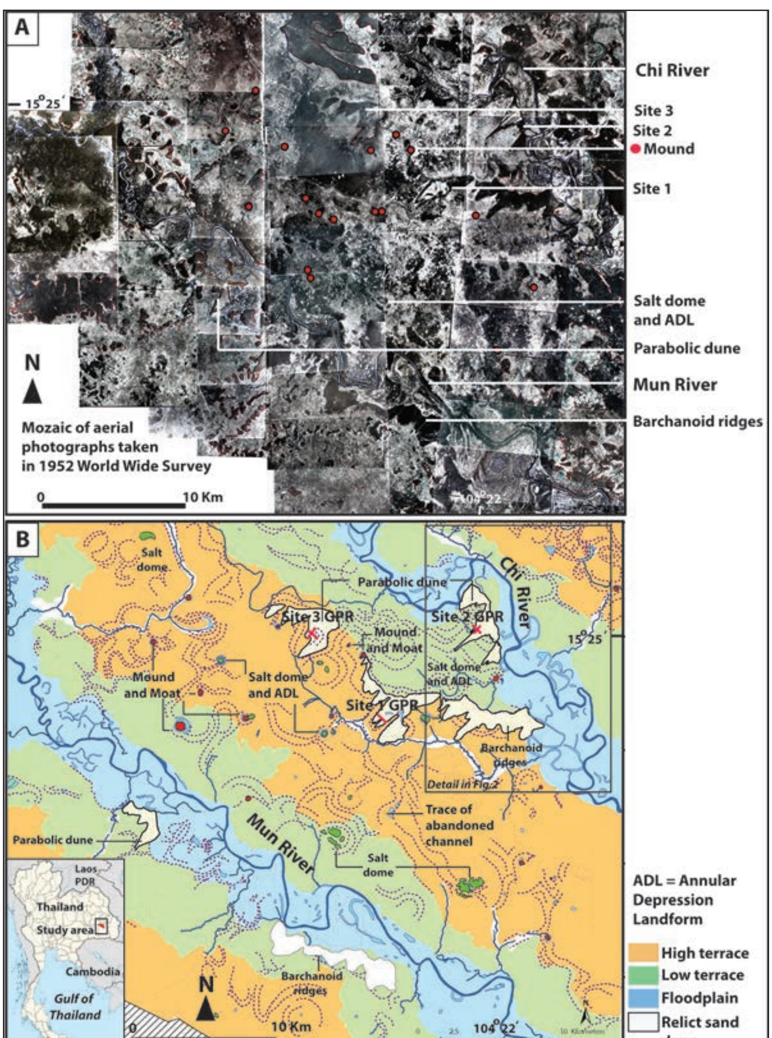

Figure 1: Map showing the study area, Thungkula Ronghai (TKR), the northeastern Thailand. (A) mosaic aerial photographs taken in 1952 used for interpreting remnants of sand dunes. Red circles are natural mound that were later classified as relict of dome dune.
(B) regional geomorphological map along the meandered belts of the Mun and Chi Rivers. Barchanoid ridges and parabolic dunes are dominated on terraces. Salt dome surrounded by annular depression landform are shown in green with dash circle.

stratigraphical records of coastal sand dune and fluvial environments (e.g. Hickin *et al*., 2009). In this paper, we hypothesized that GPR will work well in sand dune environment as the sediments have low conductivity and contain large scale sedimentary structures that can be imaged and differentiated from fluvial environment underneath. Optically stimulated luminescence (OSL) dating, one of the Quaternary geochronology techniques, that determines the time elapsed since buried sand grains were last exposed to sunlight (e.g. Huntley *et al*., 1985) was also applied in this study based on the principle that upon burial, ionizing radiation from surrounding sediment (by radioactive decay of U, Th, Rb, and K) and cosmic rays is absorbed by the mineral grains and stored in traps within their crystal lattice. OSL dating is beneficial for late Quaternary dating with the reliability of age ranging from about months to 150,000 years old with an error ranged around 5-10 % (Murray & Wintle, 2000; Murray & Olley, 2002). Calculating the age when the grain was last exposed to sunlight is based on quantifying both the radiation dose received by a sample since its zeroing event and the dose rate which it has experienced during the burial period (Dougherty *et al*., 2019). In this work, all ages are quoted in years before A.D. 1950.

Dune fields can extend from tens to hundreds of kilometers and form over long time-spans that often cover substantial changes in regional climate. It is, therefore, unclear whether the shape of dune fields that we observe today is the result of current environmental conditions (Rasmussen, 2012). Thus, in this paper, we show systematic description to answer what types of dune are preserved in this dune field, how and when they started and ceased their formation. We hypothesize that aeolian sand dunes found on the Khorat Plateau can be used as the clue of the ancient climate history and thus, may suggest that the plateau was once the desert, sometimes during the Quaternary. The discussion will focus on the formation of dune field and its relation with climate change, i.e. the dry and cold periods of the marine isotope state 3 (MIS3).

MATERIALS AND METHODS

Detailed interpretation of a series of aerial photographs from World Wide Survey (WWS) project taken in 1952 with scale 1:50,000 authorized by the Royal Thai Survey Department (Figure 1A) as well as LANDSAT satellite images taken in 2014 was carried out. The position of sand dunes was interpreted. A regional scale geomorphological map covering the middle and southern parts of TKR; Khowang district of Yasathon province and Rasi Salai district of Srisaket province was made (Figures 1B and 3B). Close up map of remnant parabolic dunes and barchanoid ridges was also produced (Figure 2). All interpreted data were registered in ArcGIS software overlying on a regional digital elevation model (DEM) for the detail geomorphological analysis.

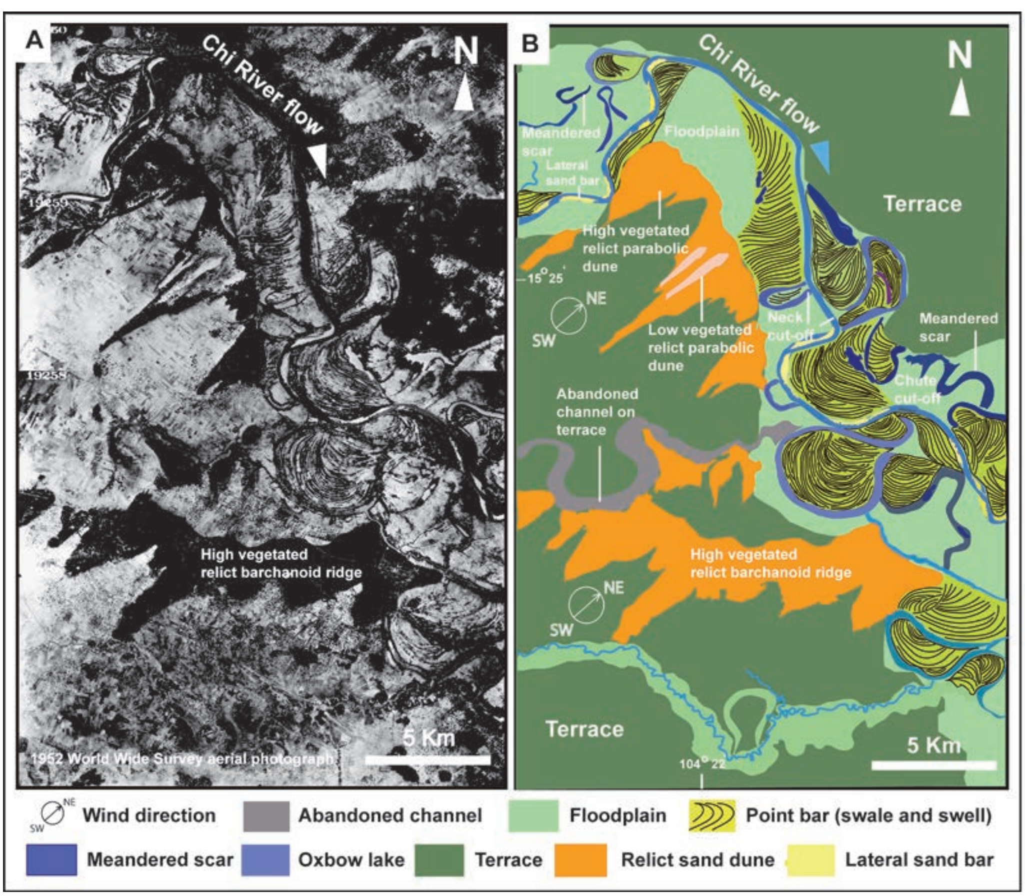

Figure 2: Close up geomorphological map of area where barchanoid ridges and parabolic dunes were studied in detail. (A) Completely-vegetated barchanoid ridges were seen clearly in 1952 aerial photographs. Compound parabolic dunes with sharp horns are shown in the upper part. Parabolic dunes here were dissected by meandering of the Chi River (also see Figures 3E and 3F). Orientation of dunes in SW-NE direction.

Grain size distribution was analyzed at every 20 cm depth from the soil layer to the below sedimentary sequence, including 25 samples. Their textural parameters including mean size, standard deviation (sorting), skewness, and kurtosis were calculated. The frequency and cumulative plots of grain size in aeolian environment from site 2 (sample no. S2C1) and site 3 (sample no. S3C1) were emphasized.

Three sites (sites 1 to 3 in Figures 1 and 2) were chosen for conducting GPR survey and collecting OSL samples due to the permission to access the sites and less vegetation that made it possible for GPR. None of the soil was formed on dune surface at all three sites. Sites 1 and 3 are located at the rim of a high terrace, whereas site 2 is situated on the low terrace closed to recent floodplain limit of the Chi River. In fact, several dunes were recognized extensively on both terrace surface of the Mun and the Chi Rivers (Figure 3B). Terrace deposits are dominated by sand derived from weathered sandstone. The massive amount of sand was possibly the source of this sand dune field.

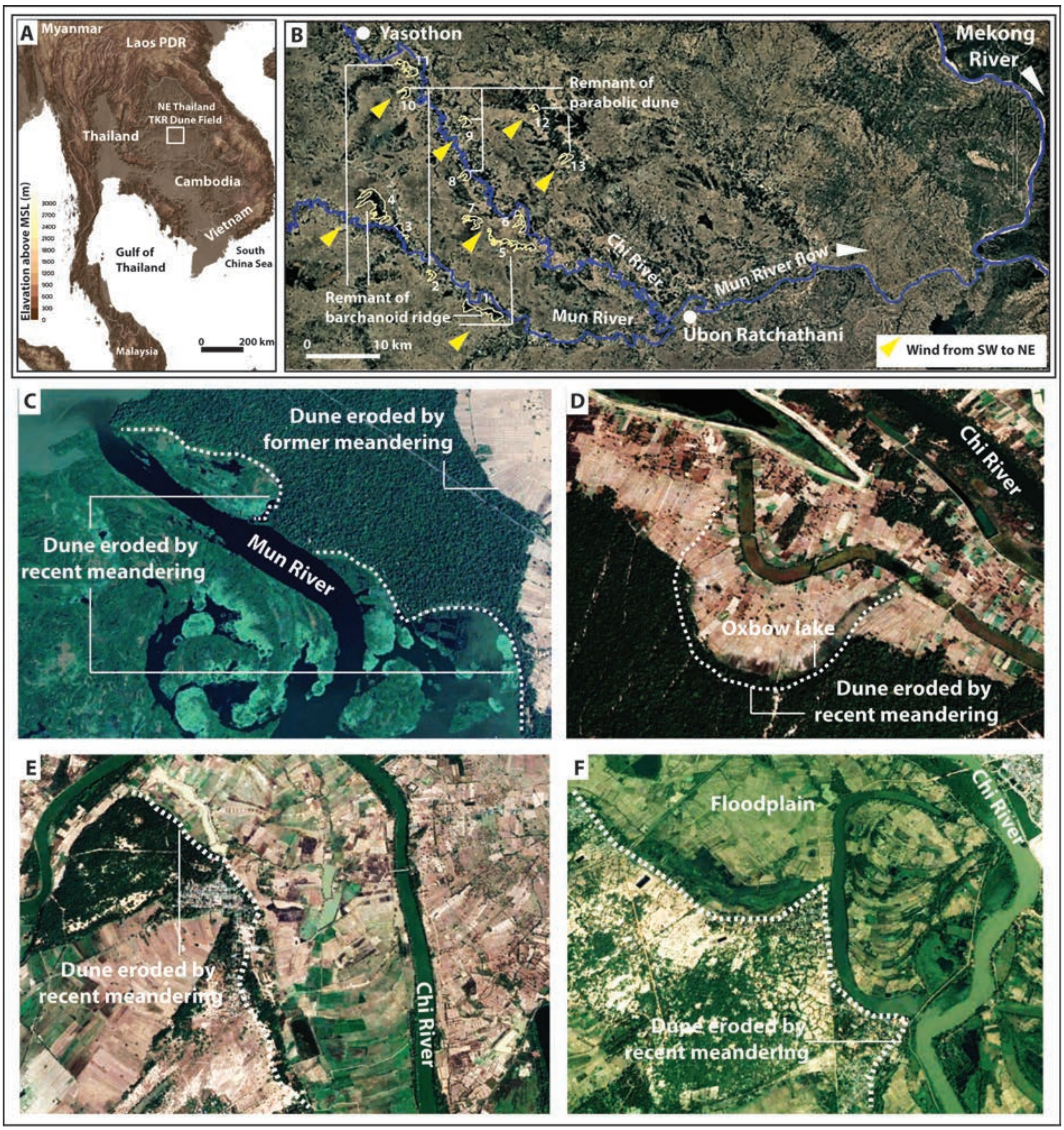

Figure 3: Index map of mainland Southeast Asia (A). (B) Spatial distribution of barchanoid ridges and parabolic dunes in TKR dune field, Yasothon and Ubon Ratchathani provinces. Yellow arrows indicate dune orientation and interpreted prevailing wind direction. (C) Example erosion of dune slip face making scarp as the boundary of modern floodplain of the Mun River. (D, E and F) Remnants of parabolic dunes that were dissected by meandering Chi River. All dunes are on low terrace.

GPR was applied to access radar facies and internal structures of the dunes. These results are further validated by some sedimentary cores taken along the traverses of GPR survey. Three sites were designed for GPR survey by using different frequency: 200 MHz and 400 MHz. Site 1 and site 3 are located on (a) remnant of barchanoid ridges and (b) parabolic dune remains on top of high and low terraces of the ancient Chi River, respectively. Site 1 GPR survey lines with 200 MHz were scanned along longitudinal and transverse transects of sand dune with a distance 200 to 300 m for interpreting paleo-channel features beneath sand dune and 400 MHz at site 3 for enhancing the internal structures of dune. In addition, the antenna 200 MHz was undertaken at site 2 for distinguishing internal sedimentary structures between recent floodplain of the Chi River and sand dunes. Raw data was processed by SIR-20 system before the interpretation in the process and formation of dunes and underneath fluvial system in correspond with stratigraphy by cores from each GPR line. Grain size analysis of dune sediment collected by hand auger along the GPR survey lines was done by sieving.

The GPR survey was undertaken at the distal part (horn) of parabolic dune with almost a flat topography remained as sand sheet or splay. The height of the dune decreases gradually from the dune crest (up to 4 m) to the horn in the distal part along the longitudinal NE to SW direction. In the transverse direction, the center of dunes is 2 to 3 m higher than the floodplain. We assigned GPR at the distal portion of dune where vegetation is a less disturbance to the internal structure of dune. First, site 1 was applied to uncover the ancient meandered belt, a fluvial feature, placed on the center of sand splay interpreted from 1952 aerial photograph (Figure 4). This area is relatively flat. Second, site 2 was carried out in the interdune located between floodplain and aeolian dune (Figure 5). Third, site 3 (Figure 6) is relatively flat similar to site 1. Signals from the GPR was classified into 6 radar facies (Table 2). A total station survey camera (Sokkia) was used to measure the topography along the GPR transects for correcting the elevation.

Chronology of sand dunes along its stratigraphy was determined by OSL. Quartz grain from sand dune samples were collected from sites 2 and 3 to infer the age of sand dunes itself and fluvial deposits. OSL sample collection, preparation and analysis were based on field and laboratory method proposed by Surakiatchai *et al*. (2019). The equivalent dose (De) measurements were carried out using a Risø TL/OSL reader (TL/OSL-DA-15) at the Department

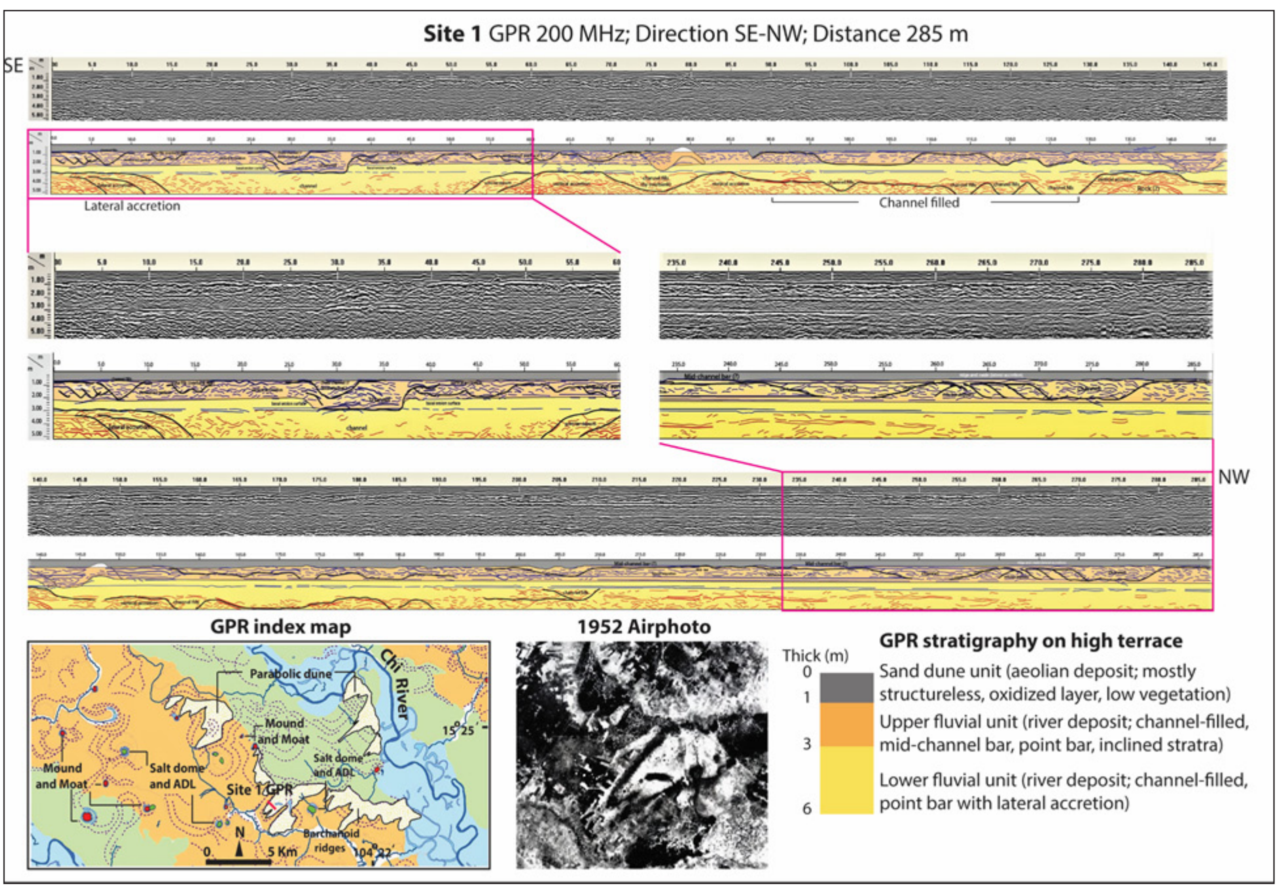

Figure 4: GPR survey on barchanoid horn at site 1 shows mostly structureless dune in the upper part of the profile. By using 200 MHz of GPR, the lower part at depth 5-6 m and the middle part (2-4 m) represents the lower and upper units of fluviatile environment. Oxidized layer beneath dune unit is the boundary contact with the fluvial deposit.

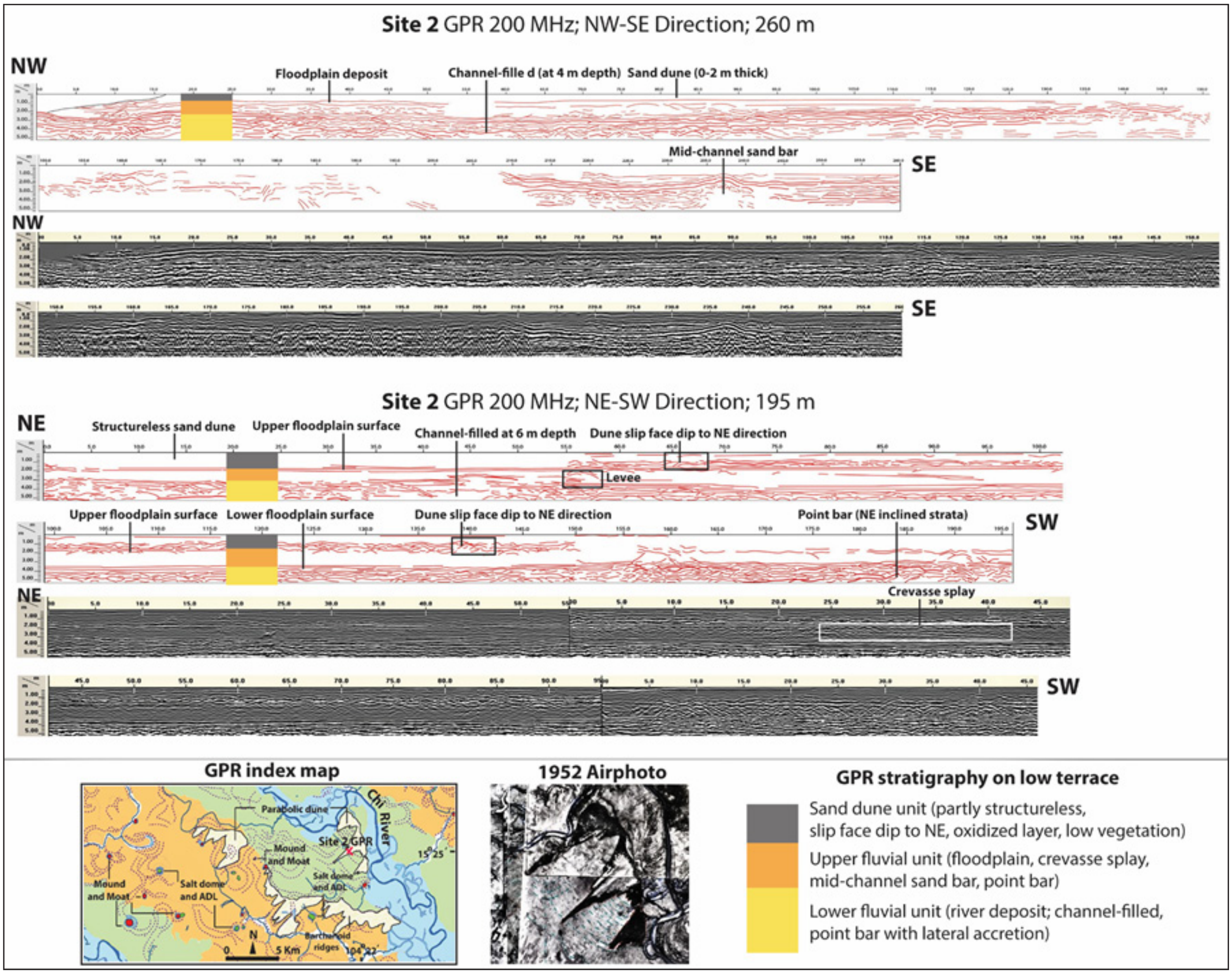

Figure 5: GPR survey with 200 MHz at site 2 shows radar facies representing different portions of meandered landforms in the lower and upper fluvial units. The boundary of upper fluvial unit and aeolian sand dune unit is obvious sharp contact. In NE-SW GPR profile, slip faces of dune dipping to NE direction are important clue of wind direction. As well, crevasse splay is recognized from the upper fluvial unit (detail explanation in text).

of Geology, Faculty of Science, Chulalongkorn University, Thailand. Each measurement was calibrated by 90Sr/90Y beta radiation source and a blue (470-720 nm) light source (Bøtter-Jensen, 1997; Bøtter-Jensen *et al*., 2000). In this OSL measurement, we used the detection filter of 7.5 mm Hoya U-340 and preheated temperature at 220 °C with the rate 5 °C/second. Prepared quartz grains were attached to a 9.8 mm diameter stainless steel disc, using silicone oil. A single-aliquot regenerative (SAR) technique (Murray & Wintle, 2003) was used for assessing all De, with test doses around 10 % of the estimated natural dose (N). The fixed test dose (usually 10–20% of the natural dose) was applied to correct any sensitivity changes. Six iterative tests were performed. In situ sand dune samples were collected for AD. In this study, AD of each sample was also derived from natural radioisotopes concentrations, i.e., U (ppm), Th (ppm), and K (%), measured by high-resolution gamma spectrometry. The gamma spectrometry was analyzed at the Department of Nuclear Engineering, Faculty of Engineering, Chulalongkorn University. In this preliminary OSL work, we inferred our result of OSL dating for the explanation of sand dune evolution in millennium scale, but the uncertainties of OSL dating results in some samples are higher than 10%. However, for further study, it should be calculated through advanced statistics (e.g. Galbraith & Roberts, 2012).

RESULTS

Classification of sand dune

Remnants of sand dunes preserved in TKR dune field were interpreted based on Pye (1993) into simple, compound and complex types (Table 1). Two major dunes remained are barchanoid ridges and parabolic dunes. The detail classification of sand dunes is as follows. First, the simple dunes (dune numbers 8, 9, 10, and 13 in Figure 3B) consist of individual dune forms which are spatially separated from their neighbors. Second, the compound type is the self-accumulated dunes that had developed by themselves. In the TKR dune field, we recognized barchanoid

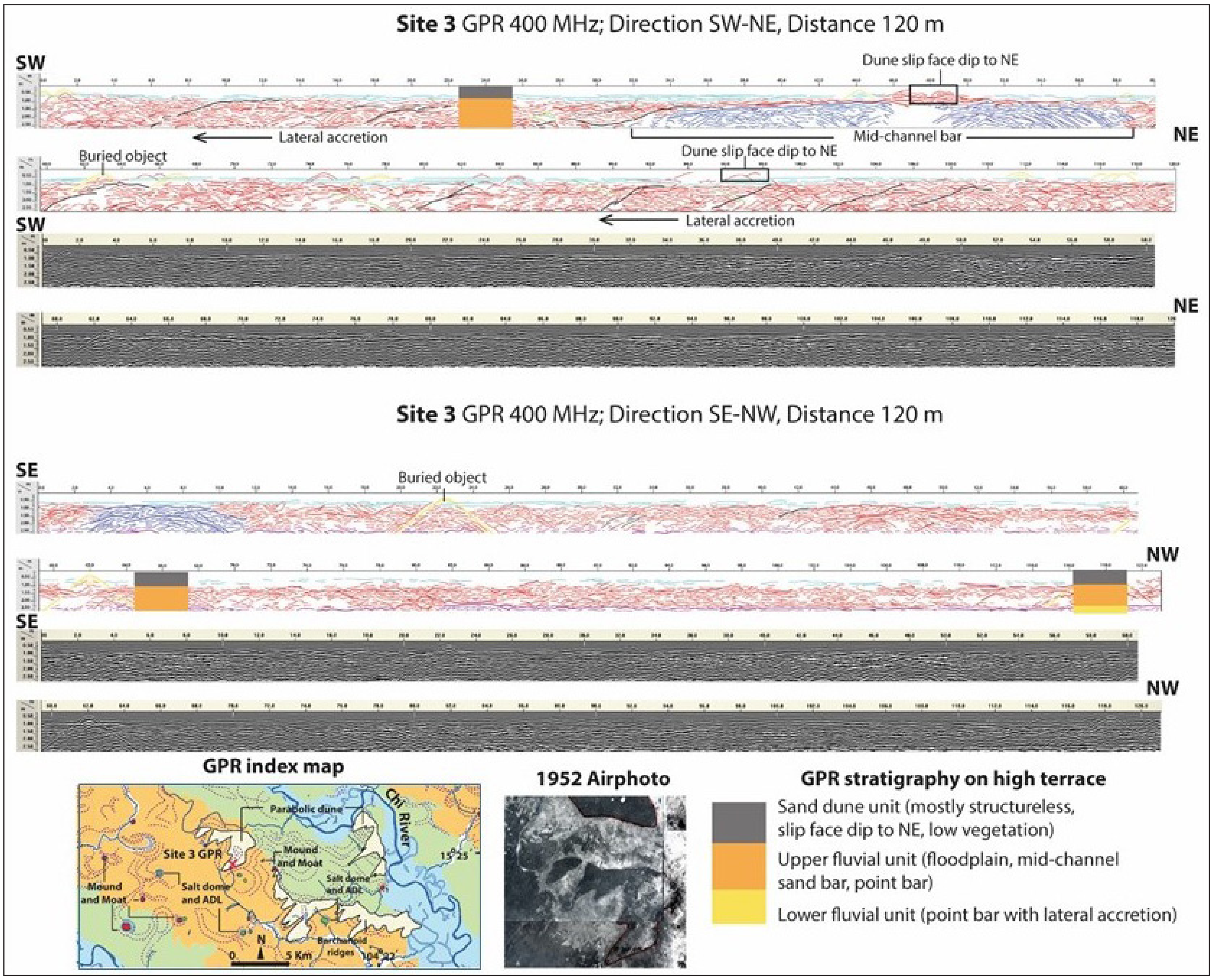

Figure 6: GPR with 400 MHz from site 3 is designed to enhance the internal structures of dune. Dune here is up to 2 m thick. Slip face is dipping to NE. Lateral accretion of point bar inclining to SW direction shows in SW-NE direction in agreement direction of paleo-channel of fluvial system beneath sand dune.

ridge (see locations of dune numbers 6 and 7 in Figure 3B and close up air-photo in Figure 2) and dome dune (red circles in Figure 1A). The compound dunes consist of two or more dunes of the same type which have coalesced or are superimposed (dune numbers 2, 4, 11, and 12 in Figure 3B). Lastly, complex dunes consist of two or more types of simple dunes which have coalesced or are superimposed (see locations of dune numbers 1, 3, and 5 in Figure 3B and close up air-photo of dune number 5 in Figure 2).

None of barchan dune was recognized in TKR dune field. The absence of barchan are maybe due to two possibilities. First, the barchan dunes have completely transformed to and made up of "megabarchanoid ridge" (a term proposed by Kar, 1990; dune numbers 1, 4, 5 in Figure 3B). Second, some of barchan dunes remained as sand sheets or small dome or mound after transformation and surface gradation by erosion. Transition of barchanoid ridges to parabolic dunes had likely occurred in this area (see location of barchanoid ridge number 5 transformed to parabolic dune number 6 in Figure 2B and model in Figure 10C) similar to the case of the modern dune environment at White Sand, New Mexico (Jerolmack *et al*., 2012). The transition is attributed to a downwind decline in sand flux caused by the development of an internal boundary layer. Decreased sand movement allows more vegetation to colonize the area between dunes, promoting the transition to parabolic dunes (Jerolmack *et al*., 2012).

Several mounds (see red circles in Figure 1A) were observed in TKR dune field. They are oval-shaped mound and consist of fine- to medium-grained sand with 1-2 m height above floodplain level. Mound surrounded by moat (see Figure 1A) is commonly interpreted as an ancient settlement site (Ngernkerd, 2017). Several mounds in TKR are not related to archeology alone, but they have been interpreted as salt dome of the Mahasarakham Formation with annular depression landform surrounding dome (see locations in Figure 1A) (Vichapan, 1992; Ngernkerd & Choowong, 2017). However, some mounds are neither salt dome nor archeological

Table 1: Classification of dune types from TKR dune field, the southern part of the Khorat Plateau, northeastern Thailand.

No.*	Location	Dimension (m)			Dune type/Description
		Length (L)	Width (W)	L/W	
1	15° 11' 24", 104° 18' 08"	2,200	2,700	0.81	Complex/hemicyclic/Barchanoid ridge consists of at least 4 hemicyclic dunes
2	15° 17' 05", 104° 08' 30"	2,640	1,070	2.47	Compound/lobate/ superimposed/Barchanoid ridges
3	15° 22' 54", 104° 05' 37"	1,080	800	1.35	Complex/lobate/Barchanoid ridges show half eroded by recent river, lee side was eroded by ancient meandered river.
4	15° 23' 58", 104° 04' 35"	5,620	1,450	3.87	Compound/en-echelon/Barchanoid ridges consist of 1 elongate shape and 2-3 lobate parabolic dunes.
5	15° 26' 39", 104° 01' 46"	1,870	475	3.94	Complex/elongate and lobate/Barchanoid ridges consist of at least 2 elongate shape and several lobate shapes (found at site 1)
		1,700	660	2.57	
6	15° 21' 40", 104° 22' 01"	3,470	1,890	1.83	Compound/lobate/Parabolic dunes transform from barchanoid ridge (found at site 2)
7	15° 24' 52", 104° 22' 22"	2,320	820	2.83	Compound/lobate/Barchanoid ridges consist of at least 2 lobate shapes forming en-echelon shape (found at site 3)
8	15° 25' 03", 104° 15' 57"	3,320	1,430	2.32	Simple/lobate/Parabolic dune
9	15° 31' 43", 104° 14' 31"	2,700	2,000	1.35	Simple/lobate/Parabolic dune
10	15° 39' 03", 104° 14' 31"	3,340	1,880	1.78	Simple/lobate/Parabolic dune
11	15° 45' 40", 104° 05' 44"	3,250	1,330	2.44	Compound/lobate/Barchanoid ridges consist of at least 2 lobate shapes
12	15° 40' 52", 104° 24' 54"	2,080	600	3.46	Compound/elongate/Barchanoid ridges formed by 2 superimposed parabolic dunes
		3,430	1,390	2.47	
13	15° 34' 05", 104° 29' 06"	1,910	400	4.78	Simple/lobate/Parabolic dune

*Dune numbers and locations show in Figure 3B. L/W ratio < 0.4 = lunate; 0.4-1.0 = hemicyclic; >1.0-3.0 = lobate and > 3.0 = elongate shape (Pye, 1993).

remains, but they may be the remnant of dome dune type. Dome dunes may form when wind velocities are low (Pye & Tsoar, 1990). Computer modeling (Parteli *et al*., 2009) suggests that dome dunes may form if the wind oscillates between two prevailing directions with a period shorter than 0.01 % of the dune's turnover time, which is the time needed for the dune to cover a distance equal to its own size. Domes may also be dunes smaller than the critical size for a barchan development where slip faces and horns are not able to evolve (Parteli, 2007). Dome dunes may transform into other dune forms. If this is the case, mounds or dome dunes at TKR has possibly transformed into barchanoid ridge (see Figure 10C).

GPR facies of remnant sand dune

Radar facies

1) Facies I: inclined reflections (IA, IB, IC)

These facies represent the migration process of sediments including slip face and lateral accretion and migration in comparison with modern lateral bar of the Chi River (Figure 7) following scroll bar, point bar and compound bar, as well as the saltation process or inland-migration dunes of aeolian deposits (e.g. Bristow *et al*., 2000; Pedersen & Clemmensen, 2005; Best *et al*., 2006; Okazaki *et al*., 2015; Srisunthorn & Choowong, 2019).

2) Facies II: free-discontinuous reflections (IIA and IIB)

This facies is interpreted as a chaotic-shaped to free-reflections in gentle dipping with low angle. The convex upward reflections are composed of discontinuous facies. They are generally observed in transverse and longitudinal sections. The facies are interpreted as crudely stratified to massive beds of fluvial or aeolian dune migration. This characteristic is suggested that the reflection-free configuration affects to lithologically undifferentiated sediment (Pedersen & Clemmensen, 2005).

3) Facies III: set of discontinuous reflections (IIIA and IIIB)

Set of discontinuous reflection of this facies group represents the isolated and mound-shaped or random reflections. It is occasionally observed in transverse section. This group is interpreted as crudely stratified to deposits related to 3-dimensional dunes or small-scale of incipient unit bars in fluvial process and feature of adhesion lamination

Table 2: Summary of GPR facies identified from remnant dunes (see text for explanation).

Radar facies			Description	Dimension (m) thickness	length	width	Interpretation	Example
I	A	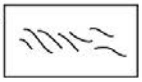	Low Inclined in sigmoidal reflections	0.6 - 1.2	-	3.0 - 7.0	Slipface and lateral migration of sediments including scorll bar, unit bar and compound bar	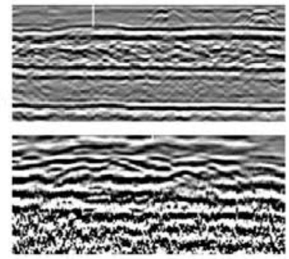
	B		Steeply Inclined dipping from top to bottom in tangential reflections	1.2 - 2.0	-	2.0 - 6.0		
	C	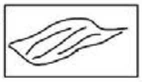	Lens shape, set of inclined in sigmoidal and oblique reflections	1.2 - 2.3	-	3.0 - 5.0		
II	A	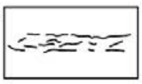	Discontinuous, chaotic-shaped to free reflections	-	-	-	Crudely stratified to massive beds of fluvial or aeolian dune migration (deflation process of aeolian sand).	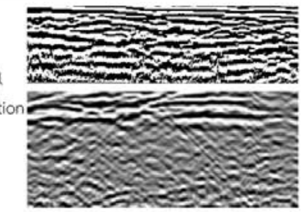
	B	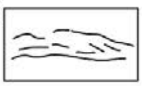	Discontinuous, inclined to low-angled and convex upward reflections	0.7 - 1.5	5.0 - 10.0	-		
III	A	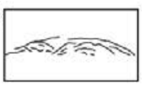	Set of discontinuous, convex reflections	3.5 - 5.2	-	3.0 - 8.0	Crudely stratified to massive beds of 3D dunes, small bars or buried objects.	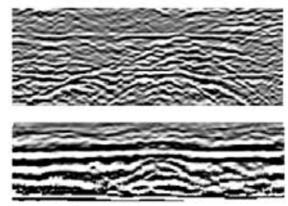
	B		Isolated, mound-shaped reflections	0.6- 1.2	-	2.0 - 3.0		
IV	A	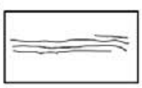	Continuous, hummocky; horizontal and parallel reflections	2.0- 4.0	<65	-	Vertical accretion in overbank deposits and water table in reflector of continuous, horizontal isolated facies.	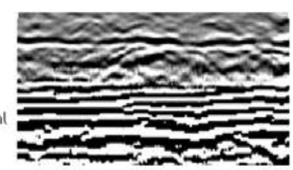
	B		Discontinuous, horizontal and parallel reflections	1.0- 2.5	<20	-		
V			Small to large-scale of channel-shaped concave-upward reflection including the assemblage of facies I - IV.	0.6- 5.0	-	4.0- 15.0	Channel fills or scour fills deposits	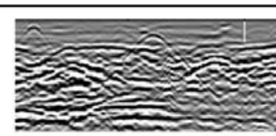
VI	A		Diffrations parabola-shaped steeping convex reflections	0.0- 0.3	-	-	The buried objects as archaeological evidences including potsherds, human remains and other artifacts.	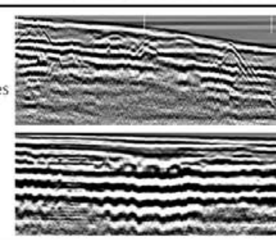
	B	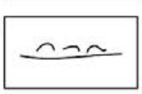	Set of small mound-shaped reflections	0.7- 1.0	-	5.0		

(i.e. adhesion wart) in aeolian sediments. Hickin *et al*. (2009) suggested this character is considered to massive deposits or a high density of sources such as buried logs.

4) Facies IV: horizontal to sub-horizontal reflections (IVA and IVB)

Horizontal reflections are continuous and parallel, rather than undulating. They appear common in longitudinal and transverse sections, but more transverse section. These facies are interpreted as stacks of vertically accreted plane beds on bar surfaces (Hickin *et al*., 2009; Okazaki *et al*., 2015). Lunt & Bridge (2004) proposed that the subparallel nature of this reflection was tended to be the successive bedload sheets deposition, as well as overbank deposits in vertical accretion of fluvial process. In addition, Pedersen & Clemmensen (2005) suggested that this appearance is

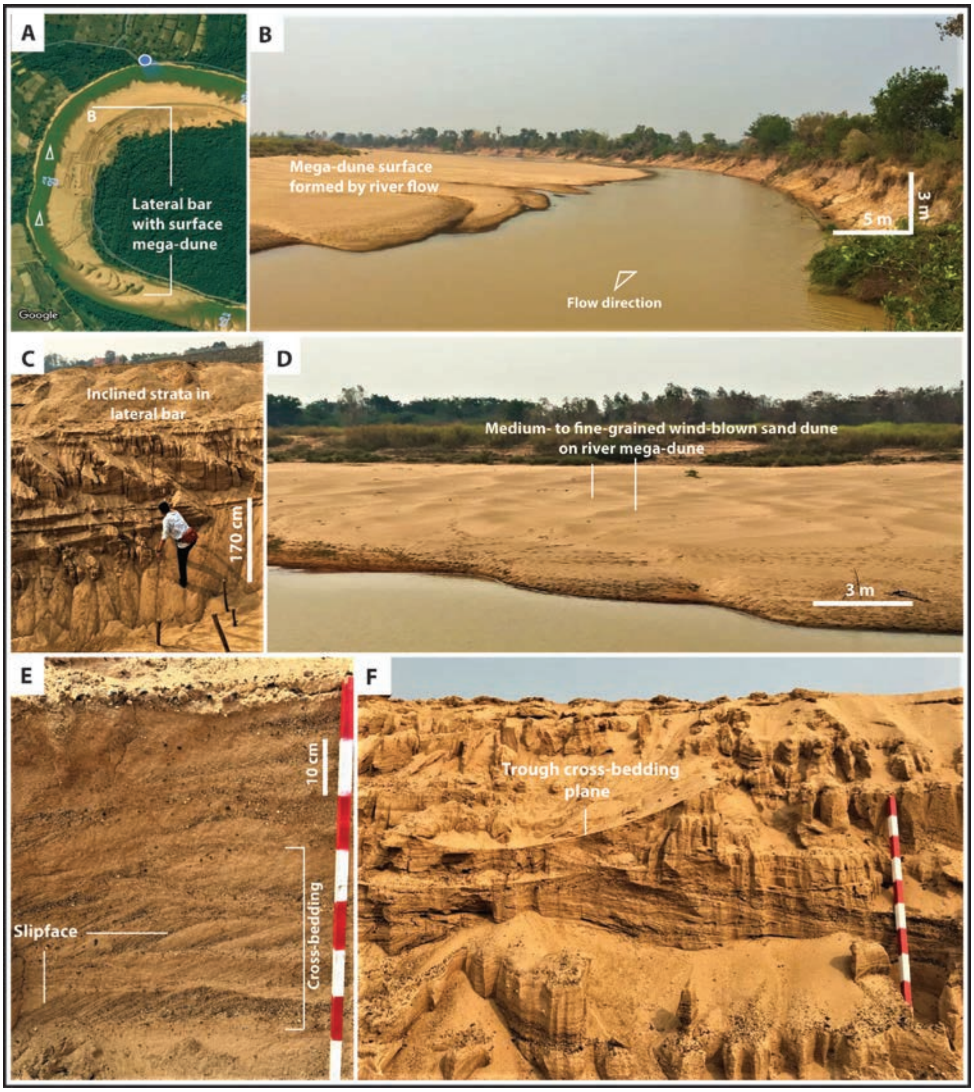

Figure 7: Recent condition of point bar in meander bend of the Chi River. (A) Google Earth image shows clearly mega-dune surface structure left behind after bank-full water flow. Water flows to the north and the River curves to the east. (B) Side view of mega-dune in lateral bar that deposits extensively that shallower of the Chi River, subsequently increases overbank flooding. (C) Inclined strata inside lateral bar with thickness up to 4 m. Large-scale incline strata indicate lateral accretion, example that can be recognized in GPR profile.
(D) Small wind-blown sand is forming on top of river mega-dune surface is one example of combination of modern processes in TKR. (E) Close-up internal structures of lateral bar including cross-bedding and slipface within mega-ripple. (F) Trough cross-bedding with point bar structure.

indicated the changes in sedimentary texture representing aeolian sand sheet environment.

5) Facies V: facies assemblage with channel-shaped lower boundary

This facies is commonly considered to represent the channel-fill deposits being the major architectural element of fluvial system (e.g. Bristow *et al*., 1999; Bridge, 2003; Best *et al*., 2006; Hickin *et al*., 2009; Nimnate *et al*., 2017a, 2017b). It is found in longitudinal and transverse sections.

6) Facies VI: diffractions of parabola-shaped reflections

Facies VI is parabola-shaped steeping convex reflections. This facies is observed at site 2 in which discovered the archaeological remains. Thus, it is related to discrete items of material culture (Duke *et al*., 2016).

Paleo-environment from GPR facies

Almost GPR data indicates that the aeolian environments overlying on fluvial environments (Figures 4-6). They are bordered by remarkable radar stratigraphy and natural break in radar facies. Fluvial environments of site 1 are divided into 2 periods including lower fluvial unit (2.9-6.0 m depth) and upper fluvial unit (0.6-2.5 m depth). Both units showed the channel fills with vertical accretion interpreted as overbank flow of channels and erosional surface or mid-channel bar (Figure 7) founded generally in meandering channel (e.g. Bristow, 1993; Bridge *et al*., 1998; Best *et al*., 2003). The uppermost layer is aeolian deposit – aeolian unit (0.0-0.6 m depth). This reflection is invisible without internal structure, therefore, it is considered as aeolian sand layer since grain size covering on surface is characterized by fine sand, well sorted and homogeneous and structureless that it is similar to pale yellow color loess (Boonsener, 1991).

However, internal structure of sand dune is clearly visible at site 2 located on floodplain of the Chi River. Ridge is parallel to the direction of prevailing wind forming in somewhere the sand supply is limited. The last upper layer of GPR profile is the aeolian environment at depth 0.0-2.5 m. The facies IA, IIA and IIB are identified as saltation process during the sediment was blown, in addition to vertical grainfall of sediments after deposition that it is related to adhesion structure. Adhesion wart is predominant at 30-40 m distance of Line 1 (NW-SE direction or transect section). This appearance indicates that the strong paleo-wind had frequently shifted direction (Kocurek & Fielder, 1982), leading to the formation of dome dunes on surface of terraces in TKR dune field. Site 3 is similar to site 1 in that sand splay layer is also found in the upper layer at 0.0-0.6 m depth without internal structure, but signals composed of gently inclined reflections in two directions interpreted as a channel feature is appeared in 46-49 m distance of GPR line.

Sediment properties of dune

Grain-size parameter of sand dune

Sand dune is obviously homogeneous with mean size of fine-grained sand (Figure 8A). They present the similarity of lined-shape in each depth range. For S2C1, the mean size is less varied from 1.90-2.14 phi that it increases at 20 cm depth from 1.90 to 2.06 phi showing the change of medium to fine-grained sand and slightly decreases at 1.20 m depth, but it raises up again at 1.80 m depth. Sorting values are around 0.69-0.89 phi (moderately sorted) and the skewness values quite change, but all values are in the range of very fine-skewed. Kurtosis values tend to continuously decrease and significantly fall at 1.20-1.60 m depth identified to extremely leptokurtic. Similarly, S3C1 results illustrate that the mean size values are more homogeneous with 2.2-2.3 phi (fine-grained sand) and sorting values are stable. It is identified as moderately sorted. Skewness is in the range of very fine-skewed. Kurtosis values are extremely leptokurtic. In addition, water content is changed together with the four parameters. It tends to increase along the depth which is predominant at 2.0 m depth related with water table.

Cumulative curves of S2C1 and S3C1 indicate the unimodal frequency curve shapes (Figure 8A). These curves reveal the transport patterns proposed by Visher (1969) including the traction population in very coarse sand and coarse sand before medium to fine sand was the most of saltation population at peak. It rarely shows the suspension population in transportation.

Scatter plot of statistical grain-size parameters

A scatter plot (in phi) measurement unit can be used to indicate the difference in sedimentary characteristics in order to distinguish the depositional environments. The bivariate plot of mean size versus sorting known as Stewart (1958) (Figure 8B) was used to provide significant clues to understand the energy conditions and formation processes at the time of deposition. The S2C1 with OSL samples in scatter plots represent that the three groups of sediment might reflect the difference of transportation and deposition processes. As well, the S3C1 scatter plots are widely scattered, but they can be separated into two groups (Figure 8C).

OSL dating

A total of 7 OSL samples were preliminary collected from dune profiles based on different physical characters of each layer at site 2 and site 3 (Figures 9A and 9B). They reveal the periods of sand dune formation (45 to 28 ka) after fluvial processes (81 to 65 ka) (Figure 9C) (Table 3). The relationship of OSL chronology and the evolution of fluvial and sand dune development will be discussed in the next sections.

DISCUSSIONS

Long-term preservation of sand dune

The remnant morphology of sand dunes in TKR dune field remains as low- and highly-vegetated area. The height of dune ridges as seen today ranges from 1 m (as in case of low or non-vegetated dune) and reaches up to 4 m as in case of highly vegetated dune (refer to dune numbers 1,4,5 in Figure 3B). Vegetation is one of the primary factors in determining parabolic dune morphology, dune length, and migration rate. Parabolic dunes form an association with vegetation and vegetation density influences dune form (Cooper, 1958). Vegetation acts to stabilize the trailing ridges of a parabolic dune and provides a general form for the individual dune (Cooper, 1958, 1967; Pye, 1982, 1983, 1993; Thompson, 1983) and by increasing the surface roughness parameter along the vegetated area (Hesp, 1981; Pye, 1983). Vegetation in parabolic dune formation can protect the less-mobile arms against the force of the wind action,

Table 3: OSL dating results of seven sand samples from pitting at Sites 2 and 3, TKR (see pitting stratigraphy in Figure 9).

Sample	Depth (cm)	U (ppm)	Th (ppm)	K (%)	W (%)	AD (Gy/ka)	AD (Error)	De (Gy)	De (Error)	Age* (ka)
2-1	90	0.42	1.71	0.15	5.54	0.44	0.10	17.33	0.38	39.5 ± 9.0
2-2	135	0.30	2.85	0.23	5.96	0.56	0.10	22.87	0.49	41.0 ± 7.4
2-3	185	0.21	3.61	0.35	5.79	0.69	0.10	30.48	0.66	44.4 ± 6.5
3-1	20	0.41	3.57	0.19	3.21	0.61	0.10	2.97	0.07	4.8 ± 0.7
3-2	50	0.22	2.87	0.15	1.91	0.49	0.10	14.18	0.31	28.7 ± 5.8
3-3	95	0.17	4.42	0.27	7.19	0.65	0.10	43.16	0.93	65.9 ± 10.0
3-4	140	0.10	4.00	0.35	4.83	0.60	0.10	49.31	1.06	81.8 ± 13.7

*All ages are quoted in years before A.D. 1950.

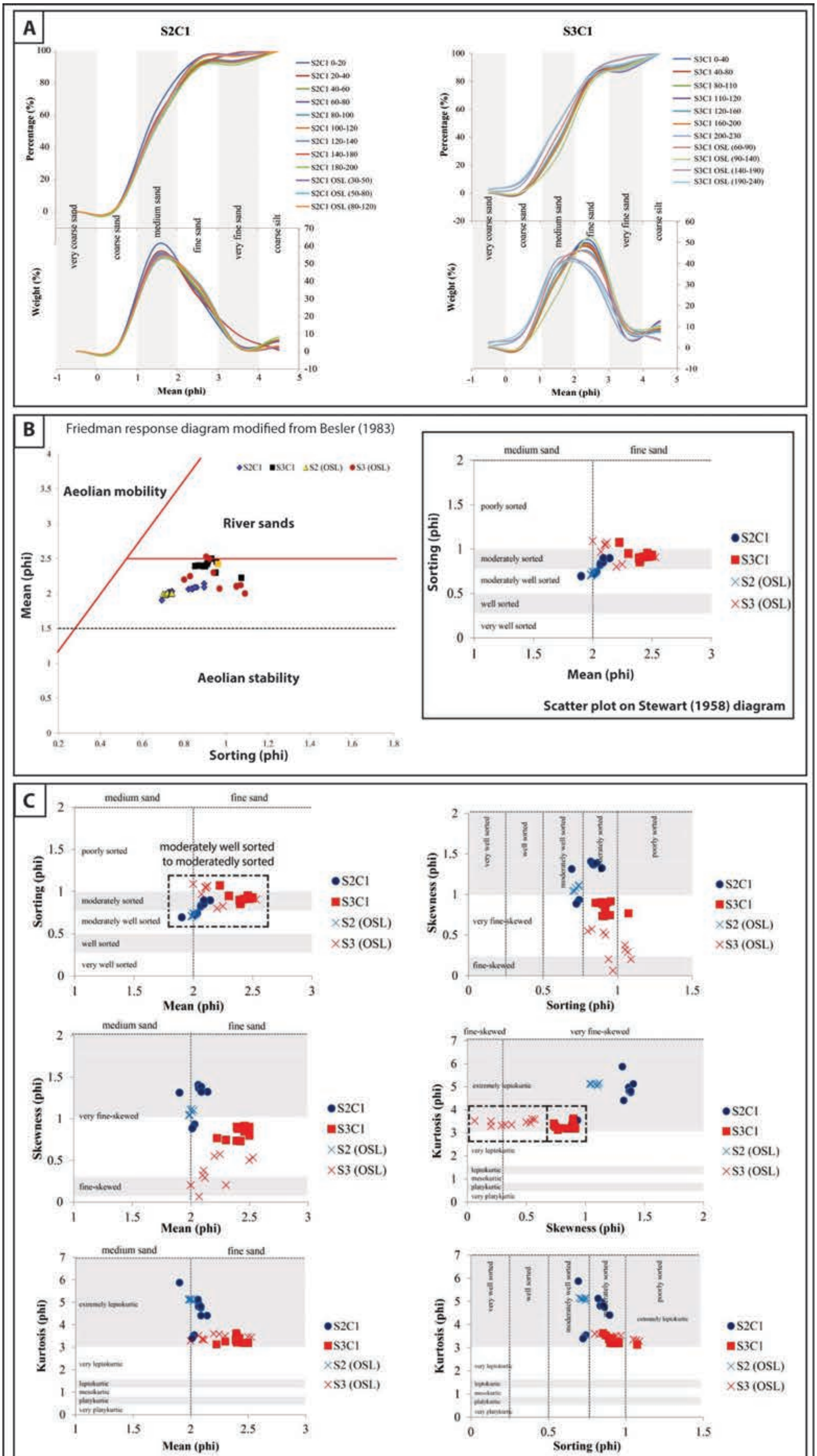

Figure 8: Grain size analysis of dune and river sands collected from cores at site 2 and site 3. (A) Distribution curve of dune sand from sites 2 and 3 showing unimodal. (B) Friedman response diagram plot of dune sand shows aeolian stability (left) and scatter plot between mean against sorting helps distinguishing dune sand from fluvial sand. (C) Various kinds of scatter plot of grain size parameters that enable to separate dune sand from river sand.

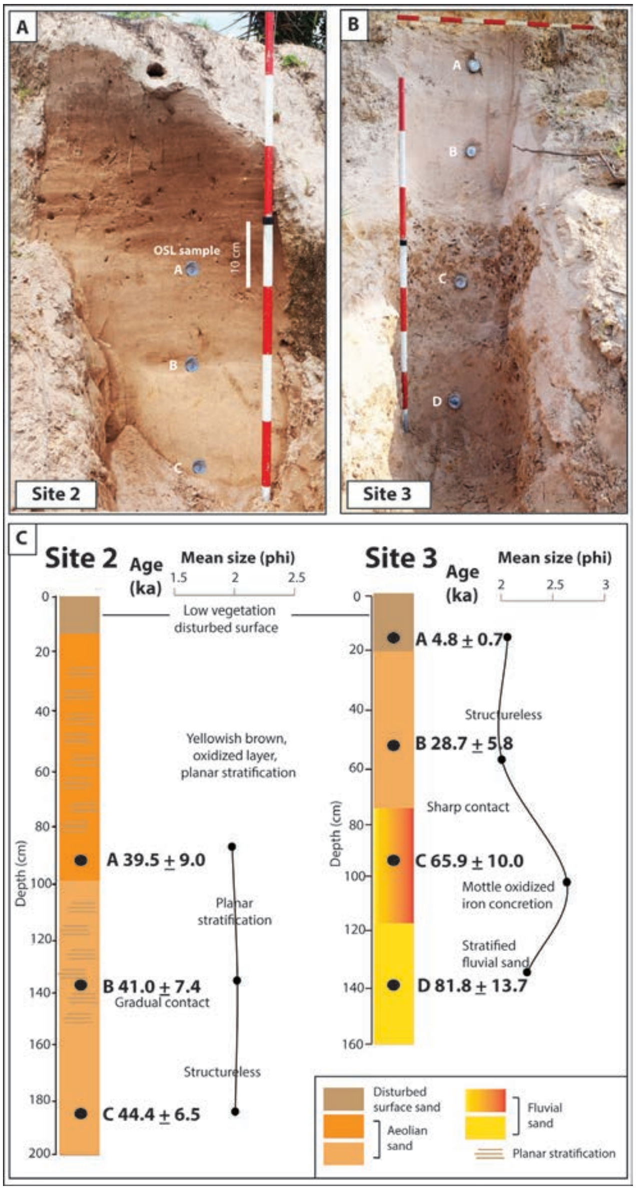

Figure 9: Geochronology and stratigraphy of aeolian and fluvial systems from site 2 and site 3. (A and B) Photographs show color difference and structures of dune and river deposits and depth of OSL samples. (C) Graphic stratigraphy and OSL age in ka. Age of fluvial deposits range from 81 to 45 ka and dune deposited between 45 to 28 ka. Youngest OSL age (4.8 ka) from site 3 indicates either reworked or local wind-blown sand splay.

thereby allowing the central part to advance downwind. The advancing apex leaves behind trailing ridges that elongate and turn the dune into a hairpin form (Tsoar, 2005) (see dune numbers 4,7,11 in Figure 3B). Also vegetation may develop within the internal area of parabolic dunes depending on the surface moisture content and water table level and if climatic conditions are suitable vegetation will completely stabilize an active parabolic dune or dune field (Cooper, 1958, 1967; Anthonsen & Jensen, 1996; David *et al*., 1999). Dunes recognized from TKR are densely vegetated (Figures 3C and 3D). This reflects long-term stability of dune possibly due to shallow level of water table from the Mun and the Chi Rivers. However, parts of parabolic dune apex and slip face of barchanoid ridges at dune numbers 3,6,7 were eroded away by meander cut bank of the Mun and the Chi Rivers (Figures 3E and 3F). Due to high physiography of salt domes from the present day floodwater, a remnant of dunes is likely suitable for ancient and recent settlements (Ngernkerd, 2017). The occurrence of sand dune cliff is the evidence of flooding caused by the long-term climate change in TKR region.

Late Pleistocene dune formation and climate conditions

In addition to being influenced by climate change, we proposed here that terrestrial aeolian sediments and remnant of dune landforms found in TKR may provide evidence for past climate changes. The other examples include loess–palaeosol sequences, as well as dune systems, now vegetated and inactive, indicating the former extent of arid conditions and past wind regimes in what are today areas of semi-arid or subhumid climates (Lancaster, 2014). The research by Cooper (1938) and Hogbom (1923) associate parabolic dune development with the climatic change at the end of the last ice age (~10 ka). With the end of the last ice age regional (central U.S. and northern Europe) precipitation increased and allowed for vegetation to anchor and eventually completely stabilize these parabolic dunes. Climatic conditions are the main factor in reactivation or stabilization of parabolic dune dunes where a change in climate and water table affects vegetation densities within the dune and can lead to reactivation of sediments or allow for an increase in vegetation growth (David *et al*., 1999).

The geochronology of sand dune from TKR was discussed based on preliminary result of OSL dating. Although the error of dating is quit high, but it provides general episodic evolution of fluvial and dune evolution. OSL age of sand dune shows its deposition from 45 to 25 ka which is correlated to marine isotope stage 3 (MIS3). However, the dune field in TKR is distributed on top of high and low terraces of the Mun and the Chi Rivers where abandoned channels were recognized extensively. GPR profiles also shows that dunes deposited on top of crevasse splay within low terrace. Slip face of dune was dissected by the recent meandering of the Chi River making dune scarp in the rim of low terrace (also see Figures 3C to 3F). Eroded dune sediments from low terrace were re-deposited in part of modern floodplain deposit at depth 10-14 m as red/yellow loess (about 8 ka) and at depth 5-9 m (about 3.5 ka) as yellow wind-blown sand (Boonsener, 1977, 1991; Udomchoke,1988). The occurrence of loess and wind-blown sand observed in floodplain stratigraphy can be interpreted that they were part of dissected dune re-deposited in floodplain after cut bank erosion by meandering process. However, the result of OSL dating expands the age of fluvial deposition continued from about 81 ka (equivalent to MIS5) (e.g. van der Kaars & Dam, 1995). Here we discuss the episodic evolution of two transition stages from fluvial environment (MIS4) prior to aeolian formation (MIS3) based on the results from geomorphological, sedimentological and chronological analyzes as follows.

Stage I: Pre-formation of TKR sand dunes (~81 to 65 ka)

Global paleo-climate had changed from wet to dry condition between 75 – 65 ka (van der Kaars & Dam, 1995; Chen *et al*., 2003; Fleitmann *et al*., 2003). OSL dating and GPR profiles revealed the pre-formation of sand dunes during 81 to 65 ka that comparatively equivalent to MIS4 of the last glacial period in the late Pleistocene. We suggested that the fluvial system was dominated in TKR during 81 to 65 ka. Overbank crevasse splay was found at site 2 located on recent floodplain of the Chi River. Change of channel bend to mid-channel bar is recognized from site 1 and site 3. Both sites are located on former floodplain of the ancient Chi River.

Crevasse splays on flood deposits are significantly shown in GPR profile of site 2. They indicated that backswamp or wetland environment was filled by overbank sand splay. In depth between 2.0-4.0 m, GPR profile in site 2 showing horizontal and sub-horizontal reflections suggested that these facies belong to vertical accretion by flood events (e.g. Miall, 1985; Bridge, 2003; Okazaki *et al*., 2015). Indeed, most of interdune characters recognized at this site are the available for wetland deposition when the water table raised up to sand dune base (Pye & Tsoar, 2009). Thus, the horizontal facies found along GPR Line 1 at 1.0-1.5 m depth were related to mottle zone (recognized in the samples from core S2C1) because of fluctuation of groundwater level at 2 m depth.

The change of channel bend was characterized from sites 1 and 3. GPR profiles illustrate the more lateral and vertical accretion such as side bar deposits, unit bar and channel fills or scour fills. These refer to the meandering channels, obviously seen on aerial photographs, and led to explain aeolian sand dune formation in 0.6-1.0 m depth. Mottle zone was founded in core S3C1. This mottle layer is a paleosol. OSL dating from this mottle layer provides the age of 65.9 ± 10.1 ka. Additionally, the bivariate plots of grain size suggested different processes between surface on center and the margin of sand dune. The sorting of sand at the margin of dune (at 0.8-1.8 m depth) ranges from poorly to moderately sorted. Grain size is fine to medium-grained sand. Therefore, this group is belonged to fluvial sediments of meandering channel that was dominated in this period. However, the top strata of fluvial sequence were possibly eroded and re-deposited during the rapid flooding of the post-deposition.

Stage II: Development of sand dunes (~45 to 28 ka)

Stage II of climate variation in this paper can be correlated to MIS3 that mean annual temperatures are higher than the Last Glacial Maximum (globally +1.7 °C for MIS3 stadial and +2.0 °C for MIS3 interstadial) (Meerbeeck *et al*., 2009). Meerbeeck *et al*. (2009) also suggested that orbital insolation forcing leads to enhanced Northern Hemisphere seasonality, with mainly warmer summers due to an increase of summer insolation, whereas winter insolation does not change substantially. Northern hemisphere mean July temperature anomalies compared to the Last Glacial Maximum are +3.5 °C for MIS3 stadial (+5.7 °C between 30° N and 90° N) and +3.8 °C for MIS3 interstadial. This MIS 3 equilibrium state is generally warmer than the Last Glacial Maximum.

Wetter condition with increase summer monsoon was observed in the interval 50 – 40 ka from the southeastern South China Sea (near Palawan Island) (Chen *et al*., 2003) and change to dry in 40 – 20 ka during the Last Glacial Maximum. It is assumed that this condition favored for decreasing river flow velocity and left behind the remains of crevasse splay, sand bar with shallow channel-fills on surface of the Mun and Chi River terrace and floodplain. Massive amounts of sand, then, were blown out by strong prevailing wind from SW direction during 45 – 28 ka based on OSL dating of sediment from aeolian sand dune layer at site 2 and site 3. In addition, the Freidman response diagram (Figure 8B) identified the sediment of site 3 as aeolian stability inferring subsequently reworked by aeolian process.

Internal sedimentary structure of sand dunes derived from GPR profiles show homogenous with pale horizontal lamination. Radar facies of IA, IIA and IIB are among important characteristics of aeolian process. They are identified to have formed by saltation process during the sediment was blown out. The pre-aeolian environment of TKR was dominated by floodplain and meandered channels, so that the adhesion structure is possibly formed. Significantly, the adhesion wart is dominated at 30-40 m distance of Line 1 at site 2. This appearance indicates that the strong paleo-wind had also frequently shifted in NW-SE direction beneath pre-existing micro-topography leading to the formation of dome dunes possibly distributed on terraces in between the Mun and Chi Rivers (Figures 10A and 10E). Nevertheless, sets of radar facies within TKR dune field were not distinctive to infer strong wind energy as common structure in broad desert dunes. This is in agreement with the assumption proposed by Penny (2001) that the temperature and precipitation changes during the Last Glacial Maximum in northeastern Thailand were not severe.

Wind direction during TKR sand dune formation (45 - 25 ka)

What was the major wind direction during MIS3 in Thailand and Southeast Asia region? The orientation of parabolic dunes and barchanoid ridges in TKR dune field

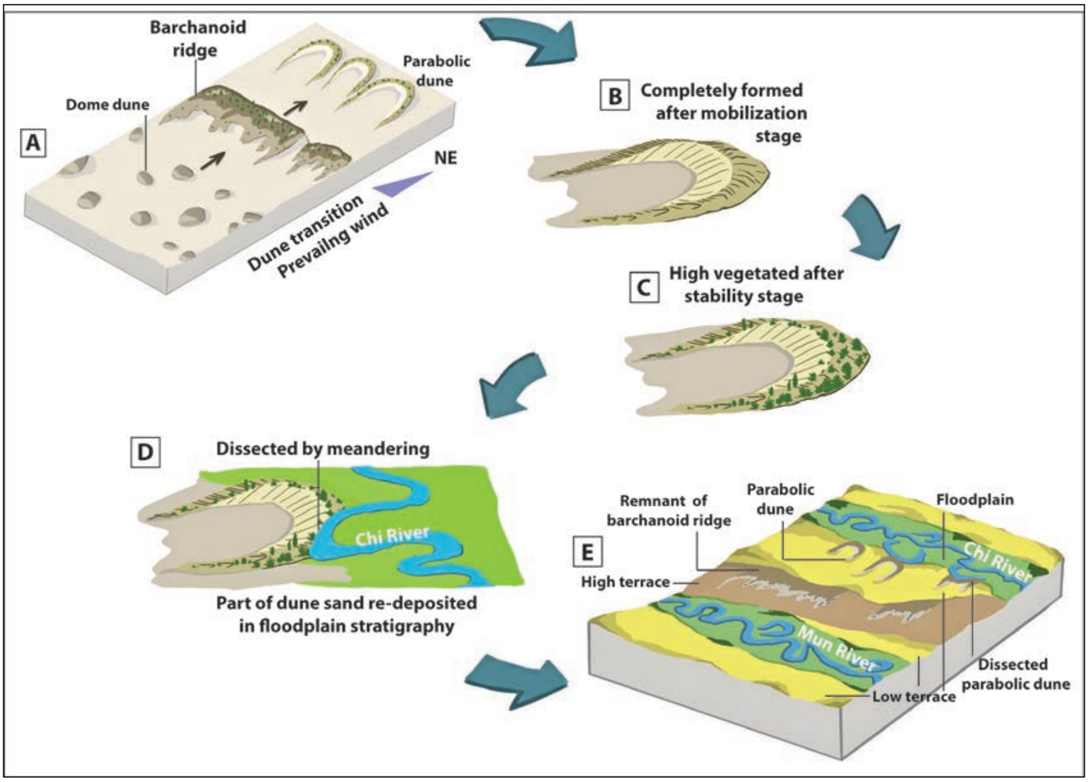

Figure 10: (A) Graphic sketch shows the proposed transformation from dome dune to barchanoid ridges and ending up to parabolic dune recognized in TKR. (B) Completely formed of parabolic dunes after mobilization. Stabilized dunes remnant include simple, compound and complex types (see text for detail explanation). (C) Vegetation started after dune stabilization stage. (D) Erosion of leeward slope by meander bend of the Chi River during meandering left behind dune scarp as the boundary of floodplain. Dune sediments were reworked to deposit in floodplain stratigraphy as previously reported (see text for explanation). (E) Block diagram illustrates recent geographical condition of the TKR where dune field was one important terrestrial geological proxy of late Pleistocene climate changes proposed in this paper.

is the clear answer. Major prevailing wind to form TKR dunes was blown from SW to NE direction. Monsoon pattern during 50 -23 ka appear to be indicated by a transitional or interstadial in which the climate was cold and humid as in case of the Chinese Loess Plateau (Li *et al*., 1988). Due to the greatly reduced size of the South China Sea (Huang *et al*., 1997), and loss of warm water input from the Indian Ocean, the summer monsoon would have been much drier (Wang & Sun, 1994; Wang *et al*., 1999). It would have approached the TKR across dry land, including the exposed shelf from southern Borneo across Indo-China to Nanning, a distance of over 4000 km over land, and would thus have been much drier than today (Nichol & Nichol, 2013). We suggest that the formation of the dune caused by the lower base level leave a vast amount of sand, which was transported by the fluvial system, on the high and low terraces.

CONCLUSIONS

Sand dunes from TKR on the Khorat Plateau, northeastern Thailand is one of rare terrestrial evidences of climate change in the late Pleistocene. It is suggested that the physiography of the Khorat Plateau favors for the preservation of climate record both warm and cold periods throughout the Quaternary. Sand dunes at TKR dune field confirmed that part of the Khorat Plateau was, once, become a local desert in the late Pleistocene. Remnants of sand dunes from TKR were identified as barchanoid ridges and parabolic dunes formed extensively by prevailing wind from SW to NE direction, i.e. SW monsoon wind. The mound or relict dome dunes were found in TKR. Massive amount of fine materials derived from surficial and weathering processes of terrace deposits became the main source to initiate the formation of dunes (dome and probably barchan types). Then, they were completely transformed to barchanoid ridges and finally to parabolic dunes (Figure 10B). Vegetation started to cover the dunes after their stabilization (Figure 10C). Part of the dunes were dissected by meandering of recent Chi River (Figure 10D). The present geomorphology in TKR is the result of avulsion and gradation that make the area become flat (Figure 10E). The remnants of sand dunes today display as undulating terrain. Relict mounds (dome dune), salt dome with the annular depression landform, archeological moat and mounds are scattered. Most of the remnant dunes consists of dense vegetation.

Apart from red/yellow loess that has been reported from the Khorat Plateau, such an old age sand dune is rarely mentioned. In the TKR region, sand dunes recognized in this paper is also limited only on the surface of the Mun and the Chi Rivers terraces. Definitely, the major source of dune sand was from those of terrace sediments that contain quartz derived from weathered sandstone beds in the lower Mun and Chi basins. GPR profiles show clearly the internal sedimentary structures of fluvial environment, but rare (mostly structureless) inside sand dunes. Only some slip faces were preserved and detected. Nevertheless, they are clear enough to help confirm the formation of dunes in SW-NE direction in correspond with the orientation of remnant shape of parabolic and barchanoid ridges.

Result of OSL dating suggested primarily the formation of dune during 45-28 ka in similar to the time of marine isotope stage 3 (MIS3). The OSL ages of fluvial deposits beneath the sand dunes revealed that the fluvial system dominated in TKR during 81-65 ka (relatively correlated with MIS4). The temperature from MIS4 is expected to decrease (colder) to MIS3 until the Last Glacial Maximum (21 ka). However, the occurrence of dunes in TKR means the breakdown of cold condition and the transition of cold and dry to warm and drier, the condition, coupled with continue prevailing wind, that favored for aeolian dune to form. This suggested that dunes in TKR, as geological proxy, can infer the interstadial during MIS3 in the Khorat Plateau and the mainland Southeast Asia. In conclusion, the finding of this work provides the challenge for further study on the record of late Pleistocene ENSO in Southeast Asia region. Such a future research could be taken into account from the other terrestrial depositions on the Khorat Plateau and the suitable environments nearby.

ACKNOWLEDGEMENTS

The 90th Anniversary of Ratchadapisek Somphot Endowment provided scholarship to P.N. National Research Council of Thailand (NRCT), and Ratchadapisek Somphot Fund of Chulalongkorn University provided the fund to M.C. Prof. S. Pailoplee (mitrearth.org) provided DEM for Figure 3A. MESA Research Unit sponsors logistic, field and laboratory expenses. The Editor and two anonymous reviewers are acknowledged for constructive comments that greatly improved the quality of the manuscript.

REFERENCES

Anthonsen, K.C. & Jensen, J.L., 1996. Evolution of a dune from cresentic to parabolic form in response to short-term climatic changes: Rabjerg Mile, Skagen Odde, Denmark. Geomorphology, 17, 63-78.

Best, J. L., Ashworth, P. J., Bristow, C. S. & Roden, J., 2003. Three-Dimensional Sedimentary Architecture of a Large, Mid-Channel Sand Braid Bar, Jamuna River, Bangladesh. Journal of Sedimentological Research, 73(4), 516-530. doi:10.1306/010603730516.

Best, J., Woodward, J., Ashworth, P., Sambrook Smith, G. & Simpson, C., 2006. Bar-top hollows: A new element in the architecture of sandy braided rivers. Sedimentary Geology, 190(1-4), 241-255. doi:10.1016/j.sedgeo.2006.05.022.

Boonsener, M., 1977. Engineering Geology of the Town of Khon Kaen, Northeast Thailand. M.Sc. thesis, Asian Institute of Technology.

Boonsener, M., 1991. The Quaternary stratigraphy of northeast Thailand. Journal of Thai Science, 1, 23-32.

Bøtter-Jensen, L., 1997. Luminescence techniques: instrumentation and methods. Radiation Measurements, 27, 749–768. doi: 10.1016/S1350-4487(97)00206-0.

Bøtter-Jensen, L., Bulur, E., Duller, G.A.T. & Murray, A.S., 2000. Advances in luminescence instrument systems. Radiation Measurements, 32, 523–528. doi.org/10.1016/S1350-4487(00)00039-1.

Bridge, J. S., Collier, R. & Alexander, J., 1998. Large-scale structure of Calamus River deposits (Nebraska, USA) revealed using ground-penetrating radar. Sedimentology, 45, 977-986.

Bridge, J. S., 2003. Rivers and floodplains: forms, processes, and sedimentary record. Journal of Quaternary Sciences, 19(6), 617-622.

Bristow, C. S., 1993. Sedimentary structures exposed in bar tops in the Brahmaputra River, Bangladesh. Geological Society Special Publication, 75, 277-289.

Bristow, C. S., Skelly, R. L. & Ethridge, F. G., 1999. Crevasse splays from the rapidly aggrading, sand-bed, braided Niobrara River, Nebraska: effect of base-level rise. Sedimentology, 46, 1029-1047.

Bristow, C. S., Bailey, S. D. & Lancaster, N., 2000. The sedimentary structure of linear sand dunes. Nature, 406, 56-59.

Chabangborn, A. & Wohlfarth, B., 2014. Climate over mainland Southeast Asia 10.5-5 ka. Journal of Quaternary Science, 29 (5), 445-454.

Chawchai, S., Liu, G., Bissen, R., Jankham, K., Paisonjumlongsri, W., Kanjanapayont, P., Chutakositkanon, V., Choowong, M., Pailoplee, S. & Wang, X.,2018. Stalagmites from western Thailand: preliminary investigations and challenges for palaeoenvironmental research. Boreas, 47(1), 367-376.

Chen, M.T., Shiau, L.J., Yu, P.S., Chiu, T.C., Chen, Y.G. & Wei, K.Y., 2003. 500,000-Year records of carbonate, organic carbon, and foraminiferal sea-surface temperature from the southeastern South China Sea (near Palawan Island). Palaeogeography, Palaeoclimatology, Palaeoecology, 197(1-2), 113-131. doi:10.1016/s0031-0182(03)00389-4.

Cooper, W., 1938. Ancient dunes of the upper Mississippi Valley as possible climatic indicators. Bulletin of the American Meteorology Society, 19, 33-45.

Cooper, W., 1958. Coastal Sand Dunes of Oregon and Washington. The Geological Society of America, Inc, Boulder. 169 p.

Cooper, W., 1967. Coastal Dunes of California. The Geological Society of America, Inc, Boulder. 131 p.

David, P., Wolfe, S., Huntley, D. & Lemmen, D., 1999. Activity cycle of parabolic dunes based on morphology and chronology from Seward sand hills, Saskatchewan. In: D.S. Lemmen & R.E. Vance (Eds.), Holocene Climate and Environmental Change in the Palliser Triangle: A Geoscientific Context for Evaluating the Impacts of Climate Change on the Southern Canadian Praires. Geological Survey of Canada, Bulletin 534, 223-238.

Dougherty, A.J., Choi, J.H., Turney, C.S. M. & Dosseto, A., 2019. Technical note: Optimizing the utility of combined GPR, OSL, and Lidar (GOaL) to extract paleoenvironmental records and decipher shoreline evolution. Climate in the Past, 15, 389-404.

Duke, B. J., Chang, N. J., Moffat, I. & Morris, W., 2016. The invisible moats of the Mun River Valley, NE Thailand: The examination of water management devices at mounded sites through ground-penetrating radar (GPR). Journal of Indo-Pacific Archaeology, 40, 1-11.

Filion, L., 1987. Holocene development of parabolic dunes in the central St. Lawrence lowland, Quebec. Quaternary Research, 28, 194-210.

Fleitmann, D., Burns, S.J., Mudelsee, M., Neff, U., Kramers, J., Mangini, A. & Matter, A., 2003. Holocene Forcing of the Indian Monsoon Recorded in a Stalagmite from Southern Oman. Science, 300 (13), 1737-1739.

Galbraith, R. F. & Roberts, R. G., 2012. Statistical aspects of equivalent dose and error calculation and display in OSL dating: an overview and some recommendations. Quaternary Geochronology, 11, 1-27.

Hack, J., 1941. Dunes of the western Navajo Country. Geography Review, 3, 240-264.

Hesp, P., 1981. The formation of shadow dunes. Journal of Sedimentological Research, 51(1), 101-112.

Hickin, A. S., Kerr, B., Barchyn, T. E. & Paulen, R. C., 2009. Using Ground-Penetrating Radar and Capacitively Coupled Resistivity to Investigate 3-D Fluvial Architecture and Grain-Size Distribution of a Gravel Floodplain in Northeast British Columbia, Canada. Journal of Sedimentological Research, 79(6), 457-477. doi:10.2110/jsr.2009.044.

Hogbom, I., 1923. Ancient inland dunes of Northern and Middle Europe. Geografiska Annaler, 5, 113-243.

Hokjaroen, S., 1989. Aeolian sand splays of Northeast Thailand: analysis using Landsat TM imagery. Paper presented at the Remote sensing, soil and water management in Northeast Thailand, Khon Kaen.

Huang, C.Y., Liew, P.M., Zhao M., Chang, T.C., Kuo, C.M., Chen, M.T., Wang, C.H. & Zhang, L.F., 1997. Deep sea and lake records of the southeast Asian palaeomonsoons of the last 25 thousand years. Earth Planetary Science Letters, 146, 59–72.

Huntley, D.J., Godfrey-Smith, D.I. & Thewalt, M.L.W., 1985. Optical dating of sediments. Nature, 313, 105–107.

Inman, D., Ewing, G. & Corliss, J., 1966. Coastal sand dunes of Guerrero Negro, Baja California, Mexico. Geological Society of American Bulletin, 77, 787-803.

Jennings, J., 1957. On the orientation of parabolic or U-dunes. Geography Journal, 123(4), 474-801.

Jerolmack, D.J., Ewing, R.C., Falcini, F., Martin R.L., Masteller, C, Phillips, C., Reitz, M.D. & Buynevich, I., 2012. Internal boundary layer model for the evolution of desert dune field. Nature Geosciences, 5, 206-209.

Kar, Amal., 1990. Megabarchanoids of the Thar their environment morphology and relationship with longitudinal dunes. Geography Journal, 156, 51- 61.

Kocurek, G. & Fielder, G., 1982. Adhesion Structures. Sedimentary Petrology, 52(4), 1229-1241.

Lancaster, N., 2014. Aeolian processes. Reference Module in Earth Systems and Environmental Sciences, 1-17.

Landsberg, S., 1956. The orientation of dunes in Britain and Denmark in relation to wind. Geography Journal, 122(2), 176-190.

Li, J., Z. Feng & L. Tang, 1988. Late Quaternary monsoon patterns on the loess plateaus of China. Earth Planetary Science Letters, 13, 125–135.

Loffler, E., Thompson, W. P. &Liengsakul, M., 1984. Quaternary geomorphological development of the Lower Mun River Basin, North East Thailand. Catena, 11, 321–330.

Lunt, I. A. & Bridge, J. S., 2004. Evolution and deposits of a gravelly braid bar, Sagavanirktok River, Alaska. Sedimentology, 51(3), 415–432. doi:10.1111/j.1365-3091.2004.00628.x.

McKee, E., 1979. Sedimentary structures in dunes. A Study of Global Sand Seas. United States Geological Survey, Washington D.C. 429 p.

Meerbeeck, C.J.V., Renssen, H. & Roche, D.M., 2009. How did Marine Isotope Stage 3 and Last Glacial Maximum climates differ? – Perspectives from equilibrium simulations. Climate in the Past, 5, 33–51.

Melton, F., 1940. A tentative classification of sand dunes its application to dune history in the southern High Plains. The Journal of Geology, 2, 113–161.

Miall, A. D., 1985. Architectural-Element Analysis: A New Method of Facies Analysis Applied to Fluvial Deposits. Earth-Science Reviews, 22, 261–308.

Murray, A.S. & Olley, J.M., 2002. Precision and accuracy in the optically stimulated luminescence dating of sedimentary quartz: a status review. Geochronometria, 21, 1–16.

Murray, A.S. & Wintle, A.G., 2000. Luminescence dating of quartz using an improved single-aliquot regenerative-dose protocol. Radiation Measurements, 32, 57–73. doi.org/10.1016/S1350-4487(99)00253-X.

Murray, A.S. & Wintle, A.G., 2003. The single aliquot regenerative dose protocol: potential for improvements in reliability. Radiation Measurements, 37, 377–381. doi.org/10.1016/S1350-4487(03)00053-2.

Nichol, J.E. & Nichol, D.W., 2013. Pleistocene loess in the humid subtropical forest zone of East Asia. Geophysical Research Letters, 40, 1978–1983. doi:10.1002/grl.50426.

Nimnate, P., Choowong, M., Thitimakorn, T. & Hisada, K., 2017a. Geomorphic criteria for distinguishing and locating abandoned channels from upstream part of Mun River, Khorat Plateau, northeastern Thailand. Environmental Earth Sciences, 76(331), 1–13.

Nimnate, P., Thitimakorn, T., Choowong, M. & Hisada, K., 2017b. Imaging and locating paleo-channels using geophysical data from meandering system of the Mun River, Khorat Plateau, Northeastern Thailand. Open Geosciences, 9, 1–14.

Ngernkerd, P., 2017. Geoarchaeology of ancient site settlement at eastern Thungkula Ronghai, Srisaket and Yasothon provinces in northeast Thailand. M.Sc. thesis, Department of Geology, Faculty of Science, Chulalongkorn University, Bangkok, Thailand. 184 p.

Ngernkerd, P. & Choowong, M., 2017. Geoarchaeology of the Thung Kula Rong-hai ancient site, Srisaket and Yasothon provinces, northeastern Thailand. The 43rd Congress on Science and Technology of Thailand (STT 43), 17-19 October 2017, Chulalongkorn University, Bangkok, Thailand.

Okazaki, H., Kwak, Y. &Tamura, T., 2015. Depositional and erosional architectures of gravelly braid bar formed by a flood in the Abe River, central Japan, inferred from a three-dimensional ground-penetrating radar analysis. Sedimentary Geology, 324, 32–46. doi:10.1016/j.sedgeo.2015.04.008.

Parry, J.T., 1990. Sand splays in northeast Thailand: analysis using Landsat-TM imagery. Proceedings of the 23rd International Symposium on Remote Sensing. Bangkok, pp. 433-442.

Parteli, E.J.R., 2007. Sand dunes on Mars and on Earth. Dissertation. Institut fur Computerphysik der Universitat Stuttgart, Germany. 170 p.

Parteli, E.J.R., Durán, O., Tsoar, H., Schwammle, V. & Herrmann, H.J., 2009. Dune formation under bimodal winds. Proceedings of Natural Academy Sciences, 106, 22085–22089.

Pedersen, K. & Clemmensen, L. B., 2005. Unveiling past aeolian landscapes: A ground-penetrating radar survey of a Holocene coastal dunefield system, Thy, Denmark. Sedimentary Geology, 177(1–2), 57-86. doi:10.1016/j.sedgeo. 2005.02.001.

Penny, D., 2001. A 40,000 year palynological record from north-east Thailand; implications for biogeography and paleo-environmental reconstruction. Palaeogeography, Paleoclimatology, Palaeoecology, 171, 97–128.

Phien-wej, N., Pientong, T. & Balasubramaniam, A.S., 1992. Collapse and strength characteristics of loess in Thailand. Engineering Geology, 32(1–2), 59–72. dx.doi.org/10.1016/0013-7952(92)90018.

Pramojanee, P., Liengsakul, M. & Engkagul, V., 1985. Grain size analysis of some sand rises and stream sediments in the northeast of Thailand in order to indicate depositional environment. Paper presented at the Geology and Mineral Resources Development of the Northeast, Thailand, Khon Kean University.

Pye, K., 1982. Morphological development of coastal dunes in a humid tropical environment, Cape Bedford and Cape Flattery, North Queensland. Geografiska Annaler, 64(3/4), 213–227.

Pye, K., 1983. Formation and history of Queensland coastal dunes. Zeitschrieft Fur Geomorphologie, Supplement 45 (May), 175–204.

Pye, K., 1993. Late Quaternary development of coastal parabolic megadune complexes in northeastern Australia. International Association of Sedimentology, 16, 23–45.

Pye, K. & Zhou, L.P., 1989. Late Pleistocene and Holocene Aeolian dust deposition in north China and the northwest Pacific Ocean. Palaeogeography, Paleoclimatology, Palaeoecology, 73, 11–23.

Pye, K. & Tsoar, H., 1990. Aeolian Sand and Sand Dunes. Unwin Hyman Ltd, London. 396 p.

Rasmussen, K.R., 2012. Flow and form. Nature Geosciences, 5, 164–165.

Srisunthorn, P. & Choowong, M., 2019. Quaternary meandering evolution and architecture of a point bar in the Mun River on the sandstone-dominated Khorat Plateau from northeastern Thailand. Quaternary International, 525, 25–35.

Stewart, H. B., 1958. Sedimentary reflections of depositional environment in San Miguel Lagoon, Baja California, Mexico. Bulletin of the American Association of Petroleum Geologists, 42, 2567–2618.

Story, R., 1982. Notes on parabolic dunes, winds and vegetation in Northern Australia. CSIRO Australian Division of Water and Land Resources, 43, 1–34.

Surakiatchai, P., Songsangworn, E., Pailoplee, S., Choowong, M., Phantuwongraj, S., Chabangbon, A. & Charusiri, P., 2019. Optically stimulated luminescence dating reveals rate of beach ridge and sand spit depositions from the upper Gulf of Thailand. Songklanakarin Journal of Science and Technology, 41, 1136–1145.

Thompson, C., 1983. Development and weathering of large parabolic dune systems along the subtropical coast of eastern Australia. Zeitschrieft Fur Geomorphologie, Supplement 45(May), 205–226.

Tirsch, D., 2014. Barchanoid ridge. In: Encyclopedia of Planetary Landforms. Springer, New York, NY. https://doi.org/10.1007/978-1-4614-9213-9_13-2.

Tsoar, H., 2005. Sand dunes. In: Hillel, D. (Ed.), Encyclopedia of Soils in the Environment. Elsevier, Oxford, 462–471.

Udomchoke, V., 1988. Quaternary stratigraphy of the Khorat Plateau area, Northeastern Thailand. Paper presented at the Correlation of Quaternary Successions in South, East and Southeast Asia, Bangkok, Thailand.

van der Kaars, W. A. & Dam, M. A. C., 1995. A 135,000-year record of vegetational and climatic change from the Bandung area, West-Java, Indonesia. Palaeogeography, Palaeoclimatology, Palaeoecology, 117, 55–72.

Vichapan, K., 1992. Photogeology and gravity survey of the annular depression landform in parts of Changwat Surin and Roi Et. MSc thesis, Department of Geology, Faculty of Science, Chulalongkorn University, Bangkok.

Visher, G.S., 1969. Grain size distributions and depositional processes. Journal of Sedimentary Petrology, 39(3), 1074–1106.

Wang, P. & Sun, P., 1994. Last glacial maximum in China: comparison between land and sea. Catena, 23, 341–353.

Wang, L., Sarnthein, M., Erlenkeuser, H., Grimalt, J., Grootes, P., Heilig, S., Ivanova, E., Kienast, M., Pelejero, C. & Pflaumann, U., 1999. East Asian monsoon climate during the late Pleistocene: high resolution sediment records from S. China Sea. Marine Geology, 156, 245–284.

Manuscript received 23 June 2020
Revised manuscript received 27 August 2020
Manuscript accepted 9 September 2020